Block-Coordinate-Descent Adaptive Robust Operation of Industrial Multi-layout Energy hubs under Uncertainty

Mehrdad Aghamohamadi
College of Science and Engineering
Flinders University
Adelaide, Australia

Amin Mahmoudi
College of Science and Engineering
Flinders University
Adelaide, Australia

John K. Ward
Commonwealth Scientific and Industrial Research Organization, CSIRO Energy Center, Newcastle, Australia

Mojtaba Jabbari Ghadi
National Energy Market Center
1414Degrees Company
Adelaide, Australia

João P. S. Catalão
Faculty of Engineering
University of Porto and INESC TEC
Porto, Portugal

***Abstract*— This paper presents an adaptive robust optimization approach to optimal operation of multi-layout energy hubs under uncertainty. In the first step, the multi-layout energy hub concept is presented and discussed comprehensively followed by its required energy management model, but in the deterministic form. In the next step, an adaptive robust optimization approach is developed for the energy management model of multi-layout energy hubs. The uncertainties of energy hub load as well as upstream energy market prices are considered through bounded intervals using polyhedral uncertainty sets. The proposed adaptive-robust multi-layout EHS optimizer (ARMEO) is developed as a tri-level min-max-min optimization problem which cannot be solved directly. To do so, column-and-constraint (C&C) technique is used to recast the tri-level model into a "min" master problem and a "max-min" sub-problem. However, the "max-min" sub-problem is still a bi-level model and cannot be solved directly. To cope, block coordinate descent (BCD) methodology is applied to the sub-problem to iteratively solve the "max-min" sub-problem. An industrial-based case study is conducted to show the effectiveness of the proposed model in 1) managing multi-layout energy hubs, and 2) provide immunized operational solutions against uncertainties. Based on the results, it is observed that the ARMEO model is subject to a higher operation cost (compared to deterministic model), however, the obtained operating solutions are immunized against the uncertainties. Moreover, it has been shown that the proposed multi-layout EHS model can provide reasonable operating solutions for all layouts of the system as a whole.**

***Index Terms*-- Energy hub, Column-and-constraint, Hybrid system, Multi-energy system, Multi-layout systems, Robust optimization.**

NOMENCLATURE

A. Indices

f/j	Index of EHS input/output energy carriers.
i	Index of energy converter units.
k	Index of energy storage systems.
t	Index of hour.
z	Index of EHS layouts.

B. Parameters

C_{ft}	Energy price f of the first layout in hour t.
$\bar{C}_{ft}$	Nominal estimated energy price f of the first layout in hour t.
$\tilde{C}_{ft}$	
C_{ft}^{dev+}	Positive deviation of $\tilde{C}_{ft}$.
C_{ft}^{dev-}	Negative deviation of $\tilde{C}_{ft}$.
$\hat{C}_{ft}^{dev+}$	Maximum positive deviation of energy price f in hour t.
$\hat{C}_{ft}^{dev-}$	Maximum negative deviation of energy price f in hour t.
$d/n/m$	Number of EHS inputs/converters/outputs.
T	Total number of operating hours.
$E_{kt}^{z^{lo}}/E_{kt}^{z^{up}}$	Maximum/minimum value of E_{kt}^{z}.
$E_{k}^{l^{z}}$	Energy loss for storage k of layout z.
L_{jt}^{z}	load j of layout z in hour t.
$\bar{L}_{jt}^{z}$	Forecast of load j of layout z in hour t.
$\tilde{L}_{jt}^{z}$	Uncertain load j of layout z in hour t.
$L_{jt}^{z\ dev+}$	Positive deviation of load j in hour t.
$L_{jt}^{z\ dev-}$	Negative deviation of load j in hour t.
N_X	Number of start-up variables in vector $\boldsymbol{X}$.
$N_{\tilde{U}}$	Number of uncertain parameters in vector $\tilde{\boldsymbol{U}}$.
N_Y	Number of operation variables in vector $\boldsymbol{Y}$.
$P_{ft}^{z^{up}}/P_{ft}^{z^{lo}}$	Maximum/minimum value of P_{ft}^{z}.
$P_{it}^{\prime z^{up}}/P_{it}^{\prime z^{lo}}$	Maximum/minimum value of $P_{it}^{\prime z}$.
$Q_{kt}^{ch^{z^{up}}}/Q_{kt}^{ch^{z^{lo}}}$	Maximum/minimum value of $Q_{kt}^{ch^{z}}$.
$Q_{kt}^{dis^{z^{up}}}/Q_{kt}^{dis^{z^{lo}}}$	Maximum/minimum value of $Q_{kt}^{dis^{z}}$.
S_{jk}^{z}	Coupling factor between load j and storage k of layout z.
SUC_{i}^{z}	Start-up cost of converter unit i of layout z.
$U_{i}^{ini^{z}}$	Initial status of converter i in hour t (1:on, 0:off).

v_{fi}^{z} Binary parameter which is 1 if i^{th} converter unit is supplied by f^{th} input energy and 0 otherwise, related to layout z.

$V_j^{SH^z}$ Value of unsupplied load j of layout z.

Y_{fit}^{z}/H_{ij}^{z} Auxiliary variable.

$\eta_{ij}^{c^z}$ Converter's efficiency between input i and output j of layout z.

$\eta_k^{ch^z}/\eta_k^{dis^z}$ Charging/Discharging efficiency of storage k in layout z.

Ψ Uncertainty budget.

C. Sets

Ξ^F Set of EHS input energy carriers.

Ξ^{HN}/Ξ^{WS} Set of "here-and-now"/"wait-and-see" variables.

Ξ^I Set of converters.

Ξ^J/Ξ^K Set of loads/storages.

Ξ^T Set of hours of the scheduling horizon.

Ξ^{UC}/Ξ^{UL} Set of uncertain prices/loads.

Ξ^{US} Set of uncertain parameters.

Ξ^z Set of EHS layouts.

D. Master Problem variables

$C_{it}^{SU^z}$ Start-up cost of converter unit i of layout z in hour t.

U_i^z Status of converter unit i of layout z in hour t (1:on, 0:off).

Λ_{I} Value of master problem.

E. Sub-problem variables

E_{kt}^{z} Energy level for storage k of layout z in hour t.

$P_{it}^{\prime z}$ Input energy to converter unit i of layout z in hour t.

P_{ft}^{z} Input energy f to layout z in hour t.

$P_{jt}^{SH^z}$

$Q_{kt}^{dis^z}/Q_{kt}^{ch^z}$ Discharging/Charging rate of storage k of layout z in hour t.

$\Lambda_{\mathrm{II}}/\Lambda_{\mathrm{III}}$ Value of first/second-stage sub-problem.

F. Vectors/Matrices

$\boldsymbol{A}, \boldsymbol{F}$ Coefficient matrices of objective function.

$\boldsymbol{C}, \boldsymbol{E}, \boldsymbol{G}, \boldsymbol{H}$ Coefficient vectors.

$\boldsymbol{X}, \boldsymbol{W}, \boldsymbol{D}$ Requirement vectors.

$\boldsymbol{P^z}/\boldsymbol{P}/\boldsymbol{L^z}/\boldsymbol{L}$ Vector of EHS input/output energy carriers of layout z.

$\boldsymbol{P'}$ Vector of EHS input energy to converter units of layout z.

$\boldsymbol{Q^{ch^z}}/\boldsymbol{Q^{dis^z}}$ Vector of storage charging/discharging rates of layout z.

$\boldsymbol{S^z}$ Storage coupling matrix of layout z.

$\overline{\boldsymbol{U}}/\boldsymbol{U^{dev+}}$ Vector of estimated/deviated uncertain parameters.

$\widetilde{\boldsymbol{U}}$ Vector of uncertain parameters.

$\boldsymbol{V^z}/\boldsymbol{\eta^z}$ EHS dispatch/efficiency matrix of layout z.

$\boldsymbol{Y^z}/\boldsymbol{C^z}/\boldsymbol{H^z}$ Auxiliary vector of layout z.

$\boldsymbol{X}_c$ Vector of obtained start-up variables in master problem to be send to sub-problem as fixed values.

$\boldsymbol{U^c}$ Vector of obtained worst-case realization of uncertain parameters in master problem.

$\boldsymbol{U^z}$ Vector of worst-case realization of uncertain parameters in second-stage sub-problem.

I. Introduction

A. Problem Description and Literature Survey

ENERGY hub system (EHS) has been introduced as a key approach to future multi-energy systems (MESs) as well as hybrid systems [1-3]. EHS is defined as an interface to efficiently model and operate MESs by employing different technologies to conditioning, converting, and storing various types of energy, such as electricity, heat, natural gas, etc. This is achieved using combined heat and power systems (CHP), transformers, power-electronic devices, compressors, heat exchangers, etc. [4-6]. EHS optimizes system efficiency by coupling energy systems, capitalizing on the advantages of different energy carriers. As such, the system's overall efficiency and reliability increases while energy consumption and system emissions decrease. For these reasons, EHS has been widely employed with different applications in industrial sector from steel works towards any type of industry with the ability of energy conversion these days. A load management model for industrial users was proposed in [7] to increase the arbitrage ability of industrial EHSs for optimal operation in a multi-energy smart grid. An automotive factory plant with multi-energy inputs was modeled through EHS concept to improve the efficiency of the energy flow by optimizing energy conversion paths in [8]. The operation cost of an industrial battery factory was minimized in [9] by optimizing the energy flow/conversion of the plant through EHS concept. In [10], an optimal scheduling model was also proposed employing EHS concept.

The employed EHS models in the mentioned studies rely on the conventional EHS concept presented by [4]. This model evaluates the multi-energy input/output as well as energy conversion/storage throughout the EHS. However, it is only capable to model EHSs with one set of multi-energy inputs and one set of multi-energy outputs which is called a single-layout EHS hereafter.

In some cases, especially in industrial sector, some MES applications contain complexities that cannot be modelled through the single-layout EHS model in [4]. These applications include but not limited to the following cases:

Case 1- Electric loads at various voltage levels (MV and LV) in industrial MESs, resulting in two-level energy conversion,

Case 2- MESs being coupled in series, i.e., a MES supplies another MES,

Case 3- Having storage systems at both input and output ports of MES,

Case 4-Employment of CHP units with different output voltages (MV and LV), etc.

Although, EHS concept can be applied to each layout of complex MESs, it can only be used to optimize the operation of each layout individually. This may be acceptable from each layout's perspective, but it is not the optimal solution for the whole plant. In fact, the optimal operating solution is determined for each layout individually, but the interactions between layouts has not been taken into consideration as the current EHS concept cannot characterize that. Moreover, in multi-layout configuration of MESs, each layout's output may have a different voltage level which becomes of importance as many industrial MESs include different voltage levels and therefore, they can be modelled by coupled sub-MESs in series. Also, consideration of renewables and battery systems can make it more complicated [11-12]. Therefore, further multi-layout MES modelling approaches are required to enable the existing EHS concept to model complex MES configurations.

Another considerable factor in modelling industrial MESs and optimizing their operation is the associated uncertainties with load,

renewables, and energy prices. Although, further multi-layout EHS concepts can enhance the optimality of MESs operation, the associated uncertainties can pose a noticeable effect of the feasibility of the operating solutions, if ignored.

To model uncertainties in MESs, several studies have conducted uncertainty modelling approaches to obtain immunized solutions against uncertainties. In [13] a scenario-based approach has been used to model the uncertainties of electricity price and distributed energy resources (RESs). A similar approach was conducted in [14-15]. These employed scenarios in scenario-based models are randomly generated through methods such as Benders decomposition [16]. However, scenario-based models require a full distributional knowledge of uncertain parameters, which may not be easily available in practice [17].

To obtain more reliable solutions, the optimal operation of an EHS was modeled through stochastic programing (SP) in [18]. SP was also employed in [19-22] to model the uncertainties through stochastic scenarios. Despite the advantages of the SP models, they are subject to a high computation time, which is due to the huge number of uncertainty scenarios. Moreover, it faces the lack of tractability, which is due to the required distributional knowledge of uncertain scenarios, especially, when several uncertain parameters are considered and a proper level of feasibility against different uncertainty realizations is required (this may not be practical in practice) [23]. Moreover, if the uncertain parameters deviate from scenarios, performance of SP cannot be guaranteed. This issue is also true for Monte-Carlo and probabilistic methods. To cope with the mentioned problems, RO has been employed in some recent studies to characterize uncertainties [24]. The advantage of RO is that it models the uncertainties by worst-case realization through bounded intervals, eliminating the need of scenario generation and distributional knowledge of the uncertain parameters. Therefore, the obtained solutions would be feasible as long as the uncertainty realizations are within the user-defined bounded intervals, which make it more reliable and practical than scenario-based and SP models in the literature.

It deserves mentioning that, SP is still a valid solution approach and compared to deterministic models, it provide more reliable solutions. Also, it is not as conservativeness as robust optimization. However, robust optimization is still subject to a smaller required data and the conservativeness can be eliminated by correct robust settings.

Several studies have focused on characterizing uncertainties in EHS operation through robust optimization. In [25] a single-stage robust optimization model has been developed for managing EHS operation. However, the model in [25] was a single-stage RO and was not capable to characterize recourse decisions which are dependent on uncertainties (detailed explanation of recourse decisions is provided in Section III). Moreover, the model of [25] was based on the single-layout EHS concept. In [26] the operation of interconnected EHSs was optimized through a single-stage RO approach which is the same approach conducted by [25]. Note that the interconnected EHS concept [26] is basically the consideration of EHSs having the same source in a grid and it does not provide optimal solutions for multi-layout EHSs. In [27], the employed RO model is a two-stage approach which considers recourse decisions to be obtained after uncertainty realizations. This means the study of [27] provides more reliable solutions compare to previous studies, however, it is not capable to characterize multi-layout energy systems. Similar studies have also been presented by [28-29].

Despite the advantages of the conducted RO models in the literature and their capabilities in modelling uncertainties in optimal operation of EHSs, further studies are required to provide exact modelling approaches for multi-layout EHSs with complex configurations under uncertainties.

B. Contributions

Contribution 1: A comprehensive and general multi-layout EHS model is proposed for managing industrial MESs with complex configurations. The proposed model is a continuation of the earlier study by authors and is inspired by the initial EHS concept developed in [4].

Contribution 2: To cope with uncertainties of energy prices and EHS loads, the proposed multi-layout EHS concept is expanded and developed into a two-stage adaptive robust optimization model. The proposed adaptive-robust multi-layout EHS optimizer (ARMEO) is developed as a tri-level min-max-min problem which is not directly solvable. Therefore, it is recast into a single-level min problem and a bi-level max-min problem through a decomposition methodology by means of the well-known column-and-constraint (C&C) technique [30].

However, the max-min sub-problem is still bi-level and cannot be solved directly. In previous robust models, duality theory was used to transform the bi-level max-min problem into a single-level solvable max problem. However, the use of duality theory limits the application of RO as it cannot involve integer/binary decision variables. In fact, e dual of a mixed-integer model is generally weak, nontrackable, and complicated [31]. To cope with this limitation, following contribution (Contribution 3) is presented:

Contribution 3: The proposed RO model employs block coordinate descent (BCD) method which approximates the worst-case realization of uncertainties by means of Taylor series instead of transforming the inner max-min problem into a single max problem by duality theory. BCD was originally devised to deal with single-level problems. By extending the application of BCD technique to solve the two-level max-min subproblem (resulted from the C&C generation technique), it is possible to avoid duality theory in solving the subproblem. The extension of BCD technique instead of duality theory eliminates the limitation in considering binary variables in the max-min subproblem. As a result, uncertainty-dependent binary variables such as EHS storage charging/discharging statuses can be obtained after uncertainty realization in the subproblem as recourse decisions, which was not applicable in previous dual-based RO. This results in more system flexibility in compensating the uncertainty effects such as sudden increase in load or energy prices.

C. Paper Organization

This paper is organized as follows: in Section II, the proposed multi-layout EHS concept is proposed as a deterministic model with no uncertainty consideration. The ARMEO model is then developed in Section III to characterize the uncertainties in optimal operation of the multi-layout EHS. Section IV is dedicated to simulations and numerical results. Finally, paper is concluded in Section V.

II. Proposed Multi-layout EHS Concept

A. Single-layout EHS Concept

The multi-layout EHS concept in this paper is inspired by the conventional EHS concept in [4]. In this section, the single-layout EHS concept in [4] is mathematically extended to develop the multi-layout EHS model. Configuration of a single-layout EHS is

given by Fig. 1. According to [4], the compact form of energy balance throughout the single-layout EHS is given as (1a).

$$\boldsymbol{L} = \boldsymbol{\eta} \cdot \boldsymbol{P'} - \boldsymbol{S} \cdot \boldsymbol{Q^{ch}} + \boldsymbol{S} \cdot \boldsymbol{Q^{dis}}; \quad (1a)$$

where,

$$\boldsymbol{P} = \boldsymbol{P'} \cdot \boldsymbol{V}; \quad (1b)$$

The extended form of (1a) and (1b) are presented by (1c) and (1d), respectively.

$$L_{jt} = \sum_{i \in \Xi^I} \left(\eta^c_{ji} \cdot P'_{it}\right) + \sum_{k \in \Xi^K} \left(S_{jk} \cdot Q^{dis}_{kt} - S_{jk} \cdot Q^{chg}_{kt}\right); \quad \forall j \in \Xi^J; \forall t \in \Xi^T \quad (1c)$$

where,

$$P_{ft} = \sum_{i \in \Xi^I} P'_{it} \cdot v_{fi}; \quad \forall f \in \Xi^F; \quad \forall t \in \Xi^T \quad (1d)$$

As it is seen in (1a)-(1d), the energy balance through EHS is formed by the Input energy being converted by converter units, charging/discharging of storage systems, and the load at the output ports of the EHS. However, this is not true for a multi-layout EHS as the input energy to a multi-layout EHS supplies the first layout and the next layouts, which includes the energy conversion and storage operation in all layouts. Fig. 2 shows a compact configuration of a two-layout EHS in which the output of layout $z-1$ also includes the input energy to layout z. As it is seen in Fig. 2, the conventional single-layout EHS concept in (1), does not provide any relation between the input energy to layout $z-1$ and any other variables in layout z. This means if the complex two-layout EHS in Fig. 2 is modeled by two different single-layout EHSs, the obtained operating solutions are only optimal for each layout, not the two-layout system as a whole. In this paper therefore, the multi-layout EHS concept is presented to provide the exact relation between the variables of each layout. The multi-layout EHS concept is then employed for successful modelling of complex multi-layout EHSs to be used for optimal operation of these systems.

B. Two-layout EHS Concept

For the sake of simplicity, we first extend the single-layout EHS concept to model a two-layout system and then extend this model for multi-layout systems. The general schematic representation of the single-layout EHS in Fig. 2 is extended in Fig. 3 to represent all EHS elements, i.e., converters, storages, inputs/outputs. In this configuration, the first layout, i.e., layout $z-1$, supplies both the load of layout $z-1$, i.e., L^{z-1}_{jt}, and the input energy to the next layout, i.e., P^{z}_{ft}. Based on the given configuration in Fig. 3 and employing the EHS energy balance constraint (1), the energy balance for both layouts $z-1$ and z is given by (2a) and (2b), respectively.

$$\boldsymbol{L^{z-1}} + \boldsymbol{P^{z}} = \boldsymbol{\eta^{z-1}} \cdot \boldsymbol{Y^{z-1}} \cdot \boldsymbol{P^{z-1}} + \boldsymbol{S^{z-1}} \cdot \boldsymbol{Q^{dis^{z-1}}} - \boldsymbol{S^{z-1}} \cdot \boldsymbol{Q^{ch^{z-1}}} \quad (2a)$$

$$\boldsymbol{L^{z}} = \boldsymbol{\eta^{z}} \cdot \boldsymbol{Y^{z}} \cdot \boldsymbol{P^{z}} + \boldsymbol{S^{z}} \cdot \boldsymbol{Q^{dis^{z}}} - \boldsymbol{S^{z}} \cdot \boldsymbol{Q^{ch^{z}}} \quad (2b)$$

where,

$$\boldsymbol{Y^{z-1}} = \boldsymbol{V^{z-1^{-1}}}; \quad , \quad \boldsymbol{Y^{z}} = \boldsymbol{V^{z-1}}; \quad (2c)$$

For the sake of simplicity, terms $\boldsymbol{\eta^{z-1}} \cdot \boldsymbol{Y^{z-1}}$ and $\boldsymbol{\eta^{z}} \cdot \boldsymbol{Y^{z}}$ are replaced by $\boldsymbol{C^{z-1}}$ and $\boldsymbol{C^{z}}$, respectively in (2d) and (2e).

$$\boldsymbol{L^{z-1}} = \boldsymbol{C^{z-1}} \cdot \boldsymbol{P^{z-1}} + \boldsymbol{S^{z-1}} \cdot \boldsymbol{Q^{dis^{z-1}}} - \boldsymbol{S^{z-1}} \cdot \boldsymbol{Q^{ch^{z-1}}} - \boldsymbol{P^{z}}; \quad (2d)$$

$$\boldsymbol{L^{z}} = \boldsymbol{C^{z}} \cdot \boldsymbol{P^{z}} + \boldsymbol{S^{z}} \cdot \boldsymbol{Q^{dis^{z}}} - \boldsymbol{S^{z}} \cdot \boldsymbol{Q^{ch^{z}}}; \quad (2e)$$

After some manipulations on (2e), $\boldsymbol{P^{z}}$ is obtained as (2f).

$$\boldsymbol{P^{z}} = \boldsymbol{H^{z}} \cdot \left(\boldsymbol{L^{z}} + \boldsymbol{S^{z}} \cdot \boldsymbol{Q^{ch^{z}}} - \boldsymbol{S^{z}} \cdot \boldsymbol{Q^{dis^{z}}}\right); \quad (2f)$$

where,

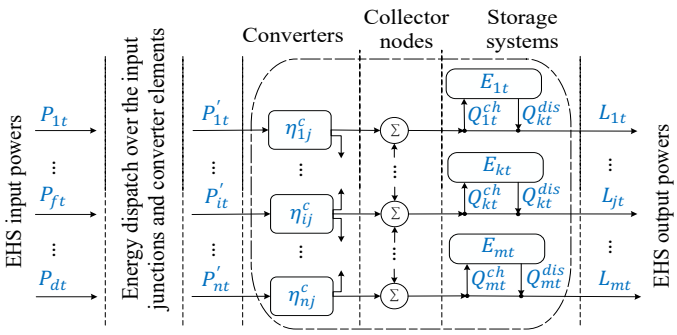

Fig. 1. General schematic representation of a single-layout EHS.

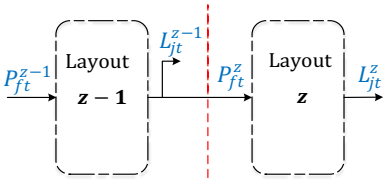

Fig. 2. Configuration of a two-layout EHS.

$$(\boldsymbol{C^{z}})^{-1} = \boldsymbol{H^{z}}; \quad (2g)$$

By replacing $\boldsymbol{P^{z}}$ in (2d), the energy flow throughout both layouts is obtained as (2h). (2h) represents the exact energy flow as well as the energy balance from the input of the first layout, i.e., layout $z-1$, to the output of the second layout, i.e., layout z.

In fact, (2h) shows how the variables of the second layout can directly affect the variables of the first layout, and alternatively, the input energy from the upstream network at the input ports of the first layout.

$$\boldsymbol{L^{z-1}} = \boldsymbol{C^{z-1}} \cdot \boldsymbol{P^{z-1}} + \boldsymbol{S^{z-1}} \cdot \boldsymbol{Q^{dis^{z-1}}} - \boldsymbol{S^{z-1}} \cdot \boldsymbol{Q^{ch^{z-1}}} - \boldsymbol{H^{z}} \cdot \left(\boldsymbol{L^{z}} + \boldsymbol{S^{z}} \cdot \boldsymbol{Q^{ch^{z}}} - \boldsymbol{S^{z}} \cdot \boldsymbol{Q^{dis^{z}}}\right); \quad (2h)$$

Considering the indexing in the general schematic representation of the two-layout EHS in Fig. 3, the energy balance equation (2h) can be extended to (2i) charactering converters, storages, and inputs/outputs on each layout.

$$L^{z-1}_{jt} = \sum_{i \in \Xi^I} \left(\eta^{c^{z-1}}_{ij} \cdot Y^{z-1}_{fit} \cdot P^{z-1}_{ft}\right) + \sum_{k \in \Xi^K} \left(S^{z-1}_{jk} \cdot Q^{dis^{z-1}}_{kt} - S^{z-1}_{jk} \cdot Q^{ch^{z-1}}_{kt}\right) - \sum_{i \in \Xi^I} H^{z}_{ij} \cdot \left(L^{z}_{jt} + \sum_{k \in \Xi^K} \left(S^{z}_{jk} \cdot Q^{dis^{z}}_{kt} - S^{z}_{jk} \cdot Q^{ch^{z}}_{kt}\right)\right); \quad \forall j \in \Xi^J; \forall t \in \Xi^T \quad (2i)$$

C. Multi-layout EHS Concept

Configuration of a multi-layout EHS is given by Fig. 4. With the same approach taken for the two-layout EHS, it is possible to model a three-layout EHS. The technique is a bottom-up approach to each two consecutive layouts. For example, for a four-layout system, we first model the last two layouts and develop the equation (2i) for it. Then we treat these two layouts as one individual layout which is added to another layout, and so on. This process has been shown in Fig. 4 by lines (the green line shows a two-layout EHS, the red line shows a three-layout EHS, the blue line shows a $z-1$-layout EHS, and the black line shows a z-layout EHS). Accordingly, the energy balance (2h) can be developed as (3a) for a multi-layout EHS containing z number of layouts.

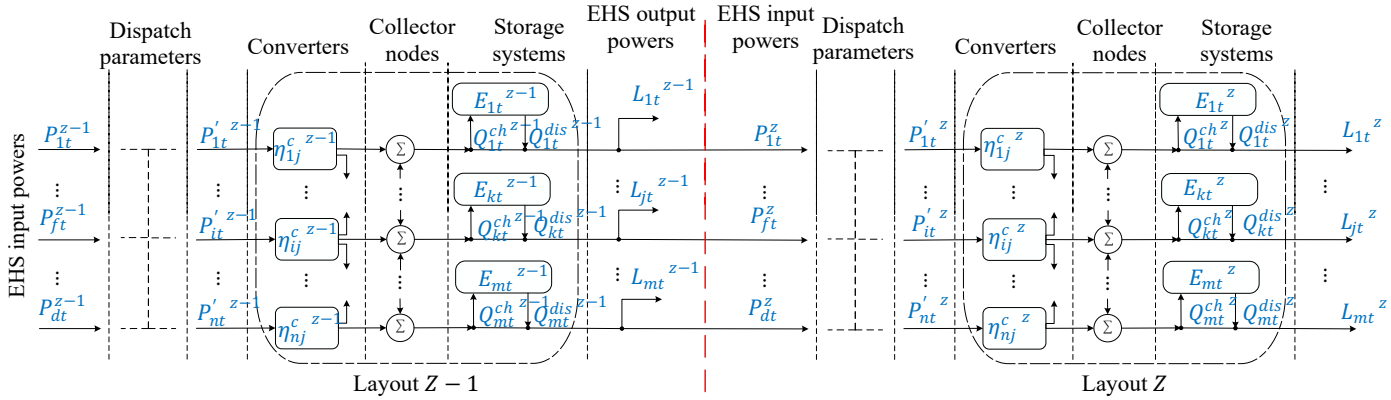

Figure 3. General schematic representation of a two-layout EHS.

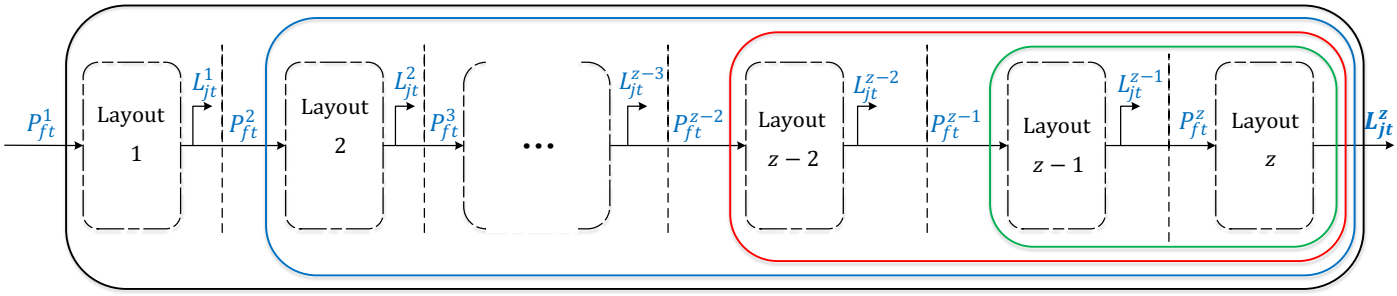

Figure 4. Configuration of a multi-layout EHS.

$$\boldsymbol{L^1 = \eta^1 \cdot Y^1 \cdot P^1 + S^1 \cdot Q^{dis^1} - S^1 \cdot Q^{ch^1} - H^2}$$
$$\cdot \Big(\boldsymbol{L^2 + S^2 \cdot Q^{ch^2} - S^2 \cdot Q^{dis^2} - H^3}$$
$$\cdot \Big(\dots \Big(\boldsymbol{L^{z-2} + S^{z-2} \cdot Q^{ch^{z-2}} - S^{z-2} \cdot Q^{dis^{z-2}} - H^{z-1}} \quad (3a)$$
$$\cdot \Big(\boldsymbol{L^{z-1} + S^{z-1} \cdot Q^{ch^{z-1}} - S^{z-1} \cdot Q^{dis^{z-1}} - H^{z}}$$
$$\cdot (\boldsymbol{L^z}) \Big) \dots \Big) \Big);$$

The energy multi-layout EHS energy balance in (3a) is expanded in (3b) to provide the exact interactions between different variables throughout all layouts. Note that, the important and the complex part of multi-layout EHS modelling is the energy balance equation between all layouts which has been obtained as (3b). Other constraints in operation optimization problem for such a system are just repetitive for each layout. For example, the allowable operating range of storage systems is the same for each storage in each layout.

$$L^1_{jt} = \sum_{i\in\Xi^I} \left(\eta^{c^1}_{ij} \cdot Y^1_{fit} \cdot P^1_{ft}\right) +$$
$$\sum_{k\in\Xi^K} \left(S^1_{jk} \cdot Q^{dis^1}_{kt} - S^1_{jk} \cdot Q^{ch^1}_{kt}\right) - \sum_{i\in\Xi^I} H^2_{ij}$$
$$\cdot \Big(L^2_{jt} + \sum_{k\in\Xi^K} \left(S^2_{jk} \cdot Q^{dis^2}_{kt} - S^2_{jk} \cdot Q^{ch^2}_{kt}\right) - \sum_{i\in\Xi^I} H^3_{ij}$$
$$\cdot \Big(\dots \Big(L^{z-2}_{jt} + \sum_{k\in\Xi^K} \left(S^{z-2}_{jk} \cdot Q^{dis^{z-2}}_{kt} - S^{z-2}_{jk} \cdot Q^{ch^{z-2}}_{kt}\right) \quad (3b)$$
$$- \sum_{i\in\Xi^I} H^{z-1}_{ij}$$
$$\cdot \Big(L^{z-1}_{jt} + \sum_{k\in\Xi^K} \left(S^{z-1}_{jk} \cdot Q^{dis^{z-1}}_{kt} - S^{z-1}_{jk} \cdot Q^{ch^{z-1}}_{kt}\right)$$
$$- \sum_{i\in\Xi^I} H^z_{ij} \cdot \left(L^z_{jt}\right) \Big) \dots \Big) \Big); \quad \forall j \in \Xi^J; \forall t \in \Xi^T$$

D. *The Deterministic Multi-layout EHS Energy Management*

The deterministic energy management model for multi-layout EHS is given by (4).

$$\min \overbrace{\sum_{t\in\Xi^T} \sum_{i\in\Xi^I} C^{SU^z}_{it}}^{\mathbb{M}1} + \overbrace{\sum_{t\in\Xi^T} \sum_{f\in\Xi^F} \left(\bar{C}^{z=1}_{ft} \cdot P^{z=1}_{ft}\right)}^{\mathbb{M}2} + \overbrace{\sum_{t\in\Xi^T} \sum_{j\in\Xi^J} \left(P^{SH^z}_{jt} \cdot V^{SH^z}_{j}\right)}^{\mathbb{M}3} \quad (4a)$$

s.t.

$$C^{SU^z}_{i(t=1)} \geq SUC^z_i \left(U^z_{i,(t=1)} - U^{ini^z}_i\right); \quad \forall i \in \Xi^I \quad (4b)$$
$$C^{SU^z}_{it} \geq SUC^z_i \left(U_{it} - U_{i,(t-1)}\right); \quad \forall i \in \Xi^I; t \in \Xi^T | t > 1 \quad (4c)$$
$$P^z_{ft} = \sum_{i\in\Xi^I} P'^z_{it} \cdot v^z_{fi}; \quad \forall f \in \Xi^F; \forall t \in \Xi^T \quad (4d)$$
$$\bar{L}^1_{jt} = \sum_{i\in\Xi^I} \left(\eta^{c^1}_{ij} \cdot Y^1_{fit} \cdot P^1_{ft}\right)$$
$$+ \sum_{k\in\Xi^K} \left(S^1_{jk} \cdot Q^{dis^1}_{kt} - S^1_{jk} \cdot Q^{ch^1}_{kt}\right) - \sum_{i\in\Xi^I} H^2_{ij}$$
$$\cdot \Big(\bar{L}^2_{jt} + \sum_{k\in\Xi^K} \left(S^2_{jk} \cdot Q^{dis^2}_{kt} - S^2_{jk} \cdot Q^{ch^2}_{kt}\right) - \sum_{i\in\Xi^I} H^3_{ij}$$
$$\cdot \Big(\dots \Big(\bar{L}^{z-2}_{jt} + \sum_{k\in\Xi^K} \left(S^{z-2}_{jk} \cdot Q^{dis^{z-2}}_{kt} - S^{z-2}_{jk} \cdot Q^{ch^{z-2}}_{kt}\right) \quad (4e)$$
$$- \sum_{i\in\Xi^I} H^{z-1}_{ij}$$
$$\cdot \Big(\bar{L}^{z-1}_{jt} + \sum_{k\in\Xi^K} \left(S^{z-1}_{jk} \cdot Q^{dis^{z-1}}_{kt} - S^{z-1}_{jk} \cdot Q^{ch^{z-1}}_{kt}\right)$$
$$- \sum_{i\in\Xi^I} H^z_{ij} \cdot \left(\bar{L}^z_{jt}\right) \Big) \dots \Big) \Big); \quad \forall j \in \Xi^J; \forall t \in \Xi^T$$

$$E_{kt}^{z} = E_{k(t-1)}^{z} + \left(\eta_k^{ch^z} \cdot Q_{kt}^{ch^z} - \frac{Q_{kt}^{dis^z}}{\eta_k^{dis^z}}\right) - E_k^{l^z}; \quad \forall k \in \Xi^K; \forall t \in \Xi^T \tag{4f}$$

$$\sum_{t \in \Xi^T} \left(\eta_k^{ch^z} \cdot Q_{kt}^{ch^z} - \frac{Q_{kt}^{dis^z}}{\eta_k^{dis^z}}\right) = T \cdot E_k^{l^z}; \ \forall k \in \Xi^K \tag{4g}$$

$$P_{ft}^{z^{lo}} < P_{ft}^{z} \leq P_{ft}^{z^{up}}; \quad \forall f \in \Xi^F; \forall t \in \Xi^T \tag{4h}$$

$$P_{it}^{\prime z^{lo}} \cdot U_{it} \leq P_{it}^{\prime z} \leq P_{it}^{\prime z^{up}} \cdot U_{it}; \ i \in \Xi^I; \forall t \in \Xi^T \tag{4i}$$

$$Q_{kt}^{ch^{z^{lo}}} \cdot x_{kt}^{ch^z} \leq Q_{kt}^{ch^z} \leq Q_{kt}^{ch^{z^{up}}} \cdot x_{kt}^{ch^z}; \ \forall k \in \Xi^K; \forall t \in \Xi^T \tag{4j}$$

$$Q_{kt}^{dis^{z^{lo}}} \cdot x_{kt}^{dis^z} \leq Q_{kt}^{dis^z} \leq Q_{kt}^{dis^{z^{up}}} \cdot x_{kt}^{dis^z}; \forall k \in \Xi^K \tag{4k}$$

$$E_{kt}^{z^{lo}} \leq E_{kt}^{z} \leq E_{kt}^{z^{up}}; \quad \forall k \in \Xi^K; \forall t \in \Xi^T \tag{4l}$$

$$0 \leq P_{jt}^{SH^z} \leq L_{jt}^{z}; \quad \forall j \in \Xi^J; \forall t \in \Xi^T \tag{4m}$$

$$x_{kt}^{ch^z} + x_{kt}^{dis^z} \leq 1; \quad \forall k \in \Xi^K; \forall t \in \Xi^T \tag{4n}$$

The objective function in (4a) includes three terms. In (4a), $\mathbb{M}1$ minimizes the start-up cost of energy converters, $\mathbb{M}2$ minimizes the cost of input energy carriers at the input ports of the first layout, and $\mathbb{M}3$ minimizes the cost of unsupplied energy at EHS output ports. The objective function (4a) is subject to the constraints (4b)-(4n). The start-up cost of converters is limited by constraints (4b) and (4c). Note that, the start-up cost and the terms $\mathbb{M}2$ and $\mathbb{M}3$ are applied to all layouts (z can have any value). (4d) expresses the relationship between input energy to each EHS layout z and the input energy to the converters of the layout. The energy balance throughout all layouts is given by (4e). Constraint (4f) represents the dynamic energy balance of each storage k over time while (4g) guaranties the end-coupling operation of the storages. End-coupling constraint makes sure that the final available energy in each storage at the final time period of operation is the same as the initial available energy at the start of the operation. Therefore, each storage has enough energy balance for the next operating horizon. Constraints (4h) and (4i) limit the EHSs' input energy and converters' input energy to their allowable ranges, respectively. The charging and discharging rate of storages in each layout are limited to their allowable ranges in (4j) and (4k), respectively. The same limitation for allowable ranges is also applied to the energy level of storages and the unsupplied load in (4l) and (4m), respectively. Constraint (4n) makes sure that each storage only operates in one mode, i.e., charge or discharge.

As it is seen in (4), the energy prices C_{ft} as well as EHSs' loads L_{jt}^1, L_{jt}^2, L_{jt}^{z-2}, L_{jt}^{z-1}, and L_{jt}^{z}, are replaced by their forecast values as $\bar{C}_{ft}$ and $\bar{L}_{jt}^1$, $\bar{L}_{jt}^2$, $\bar{L}_{jt}^{z-2}$, $\bar{L}_{jt}^{z-1}$, and $\bar{L}_{jt}^{z}$, respectively. This is because, the proposed model in (4) is developed as a deterministic model which does not characterize uncertainties. Accordingly, if any of uncertain parameters deviates from its forecasted value, the obtained solutions from solving the model (4) becomes infeasible.

To avoid this, the ARMEO problem is developed in the next section.

III. The Proposed Adaptive Robust Multi-layout EHS Optimizer

In this section an adaptive robust methodology is taken to approach the operation optimization problem (4).

A. Uncertainty Set Realization

The uncertainties associated with load and energy prices are considered by bounded intervals through polyhedral uncertainty sets as (3). The uncertain parameters $\tilde{C}_{ft}$, $\tilde{L}_{jt}^1$, $\tilde{L}_{jt}^2$, $\tilde{L}_{jt}^{z-2}$, $\tilde{L}_{jt}^{z-1}$, and $\tilde{L}_{jt}^{z}$, in (5), are allowed to deviate from their nominal estimated values $\bar{C}_{ft}$, $\bar{L}_{jt}^1$, $\bar{L}_{jt}^2$, $\bar{L}_{jt}^{z-2}$, $\bar{L}_{jt}^{z-1}$, and $\bar{L}_{jt}^{z}$ in positive and negative directions which is shown by (5a) and (5b). The considered deviations are limited to their user-defined allowable ranges through constraints (5c)-(5d). The number of uncertain parameters pertaining to load and energy prices is determined by uncertainty budget Ψ in (5e). if $\Psi = 0$, no uncertain parameter can deviate from its estimated value, resulting in a deterministic model. By increasing the uncertainty budget, a greater number of uncertain parameters are allowed to deviate. The highest value for Ψ is equal to the total number of uncertain parameters, allowing all uncertain parameters to deviate from their nominal estimates.

$$\Xi^{UL} = \left\{\tilde{L}_{jt}^{z} = \bar{L}_{jt}^{z} + L_{jt}^{z\,dev+} - L_{jt}^{z\,dev-}; \forall j \in \Xi^J; \forall t \in \Xi^T; \forall z \in \Xi^Z\right\} \tag{5a}$$

$$\Xi^{UC} = \left\{\tilde{C}_{ft} = \bar{C}_{ft} + C_{ft}^{dev+} - C_{ft}^{dev-}; \quad \forall f \in \Xi^F; \forall t \in \Xi^T\right\} \tag{5b}$$

$$0 \leq L_{jt}^{z\,dev\pm} \leq \hat{L}_{jt}^{z\,dev\pm}; \ \forall j \in \Xi^J; \forall t \in \Xi^T \tag{5c}$$

$$0 \leq C_{ft}^{dev\pm} \leq \hat{C}_{ft}^{dev\pm}; \ \forall f \in \Xi^F; \forall t \in \Xi^T \tag{5d}$$

$$\Xi^{US} = \left\{\Xi^{UL} \cup \Xi^{UC}, \sum_{t \in \Xi^T} \sum_{j \in \Omega^J} \left|\frac{L_{jt}^{z\,dev+}}{\hat{L}_{jt}^{z\,dev+}} + \frac{L_{jt}^{z\,dev-}}{\hat{L}_{jt}^{z\,dev-}}\right| + \sum_{t \in \Xi^T} \sum_{f \in \Omega^F} \left|\frac{C_{ft}^{dev+}}{\hat{C}_{ft}^{dev+}} + \frac{C_{ft}^{dev-}}{\hat{C}_{ft}^{dev-}}\right| \leq \Psi\right\}; \tag{5e}$$

B. The Proposed ARMEO Problem

Two main decisions are made in RO, including "here-and-now" decisions, which are obtained before any uncertainty realizations, and "wait-and-see" decisions, which are obtained after the realization of uncertain parameters. In this study, the converters' start-up binary variables (i.e., U_{it}) are considered as "here-and-now" decisions, while other variables including EHS facilities' operation and input energy carriers are determined as "wait-and-see" decisions. This is due to the fact that, the start-up cost variables are not dependent on short-term operation of the system and therefore, they are not dependent on short-term operational uncertainties such as demand and price uncertainties. However, the battery operation as well as all other short-term operational decisions are dependent on uncertainties.

The proposed adaptive robust model is expressed through a tri-level min-max-min optimization problem as (6).

$$\min_{\boldsymbol{X} \in \Xi^{HN}} \left(\boldsymbol{A'} \cdot \boldsymbol{X} + \max_{\tilde{\boldsymbol{U}} \in \Xi^{US}} \min_{Y \in \Xi^{WS}} \boldsymbol{F'}, \boldsymbol{W}\right) \tag{6a}$$

s.t.

$$\Xi^{I} = \{\boldsymbol{X} \in \{\boldsymbol{0}, \boldsymbol{1}\}^{N_X} \mid \boldsymbol{CX} \geq \boldsymbol{D}\} \tag{6b}$$

$$\Xi^{II} = \left\{\boldsymbol{Y} \in \mathbb{R}^{N_Y} \mid \boldsymbol{E}(\boldsymbol{X}, \boldsymbol{W}, \tilde{\boldsymbol{U}}) \geq 0\right\} \tag{6c}$$

$$\Xi^{US} = \left\{\tilde{\boldsymbol{U}} \in \mathbb{R}^{N_{\tilde{U}}} \mid \tilde{\boldsymbol{U}} = \bar{\boldsymbol{U}} + \boldsymbol{U^{dev+}}\right\} \tag{6d}$$

In (6a), the outer min problem minimizes the term $\boldsymbol{A'} \cdot \boldsymbol{X}$ over "here-and-now" variables denoted by vector $\boldsymbol{X}$. This term represents $\mathbb{M}1$ in (4a) as the only dependent term on start-up variables to be obtained before any uncertainty realizations. The outer min problem is subject to constraint (6b) which represents the set of constraints (4b)-(4c) as the start-up constraints. The inner min problem in (6a) minimizes the term $\boldsymbol{F'}, \boldsymbol{W}$ over "wait-and-see" variables, while the inner max problem maximizes it over the uncertain parameters. The term $\boldsymbol{F'}, \boldsymbol{W}$ represents the set of the

remaining terms in (4a) (i.e., $\mathbb{M}2$-$\mathbb{M}3$) which are dependent on "wait-and-see" variables including EHS operation and energy flow variables. Therefore, the inner min problem is subject to constraints (4d)-(4n), represented by (6c), while, the inner max problem is subject to uncertainty set realizations as (6d) which is the compact form of (5a)-(5e).

A decomposition methodology is employed to decompose the tri-level min-max-min problem into a single-level min problem and a bi-level max-min problem by means of column-and-constraint generation technique [27]. The single-level min problem is called "master problem" and the bi-level max-min problem is called "sub-problem", hereafter.

C. *Solution Methodology to Solve the Tri-level Robust Model through Block Coordinated Descent Method*

The solution methodology includes two iterative loops namely the inner loop and the outer loop as depicted by Fig. 5. The compact mathematical formulations of master problem and sub-problem are given in Fig. 5, as per the notations in nomenclature. The outer loop in Fig. 5 is shown by red arrows while the inner loop is shown by green arrows. In the following the role of each loop is described.

Outer loop

The outer loop is responsible for transferring the obtained "here-and-now" variables from master problem to sub-problem (prior to uncertainty realizations) on one hand and submitting primal cutting planes from sub-problem to master problem, on the other hand. The sub-problem is then solved given the obtained "here-and-now" variables to determine "wait-and-see" variables and the worst-case realization of uncertain parameters to be send back to master problem in the next iteration. Therefore, a complete set of primal cuts are added to master problem in each iteration and "here-and-now" variables are updated to be sent to sub-problem. This procedure iterates through the outer loop till the convergence criteria is met (values of master and sub-problem become sufficiently close) which terminates the outer loop, and the robust solution is obtained.

Inner loop

Since, the sub-problem is a bi-level max-min problem, it cannot be solved directly. In previous robust models such as [25-29], it was recast into a single-level max problem using duality theory which limits the application of RO. This is because no binary variable can be considered in the inner max-min problem as recourse decisions – dual of a mixed integer model is generally weak, non-tractable and complicated [31]. An example of these binary variables is the storage charging/discharging status that needs to be obtained after uncertainty realizations to compensate the shortage/surplus of energy due to uncertainties of load. However, this is not applicable through conventional dual-based robust models.

In the proposed robust model in this paper, BCD method is used to solve the sub-problem through an iterative methodology instead of transforming it to a single-level problem by duality theory. As a result, there is no limitation in considering binary variables in the inner max-min sub-problem. Therefore, the storage charging/discharging status variables can be obtained after uncertainty realizations in the inner max-min sub-problem resulting in realistic and optimal solutions compared to those of the conventional dual-based robust models.

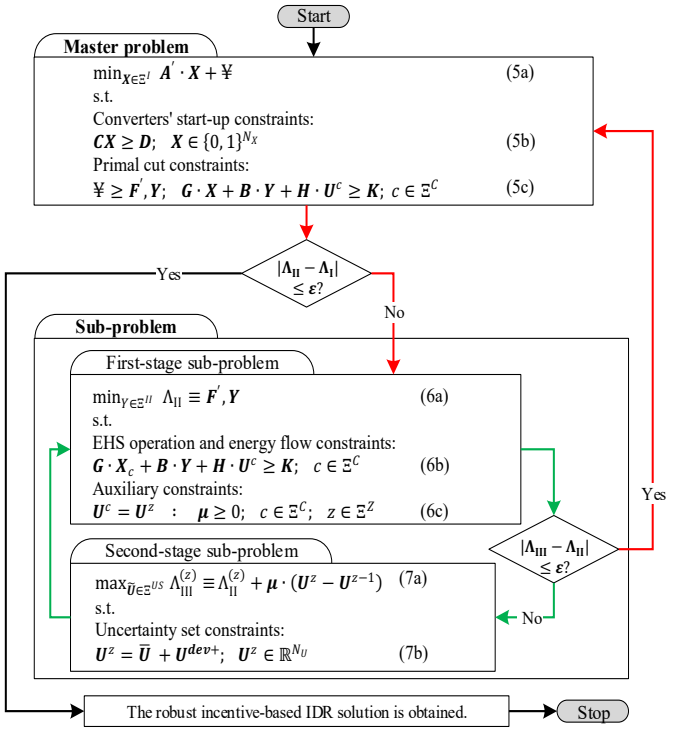

Fig. 5. Outline of the proposed two-stage BCD robust approach.

Using the BCD methodology, the sub-problem is recast into a first-stage sub-problem (characterizing the inner min problem), and a second-stage sub-problem (characterizing the inner max problem). The second-stage sub-problem is built upon the first order Taylor series approximation of uncertain parameters in the first-stage sub-problem. The first-stage sub-problem determines the "wait-and-see" variables considering the worst-case realization of uncertain parameters obtained in the second-stage sub-problem, considering the obtained "here-and-now" variables from master problem. The second-stage sub-problem is then solved to update the worst-case realization of uncertain parameters, considering the obtained "wait-and-see" variables in the first-stage sub-problem. This iterative procedure is executed through the inner loop.

Therefore, in each iteration of the outer loop, the inner loop is executed till it converges (the value of first and second-stage sub-problems become sufficiently close).

IV. Numerical Study

A. *Data Set*

Fig. 6 shows the case study which includes a three-layout EHS. The associated characteristics of each layout are also presented in Fig. 6. All inputs and outputs are in per unit (p.u.) with the base value of 100 kW. The price for input electricity to the first layout is in TOU rate with 5.3 $/p.u., 8 $/p.u., and 13.2 $/p.u., for valley, off-peak, and peak periods. Hours 01-06, 07-14/21-24, and 15-20 pertain to valley, off-peak, and peak periods, respectively. The price for input gas to the first layout is 8 $/p.u. flat rate. The load data for each layout is given by Fig. 6 (Fig. 7A, 7B, and 7C correspond to loads of layout 1, 2, and 3, respectively). These layouts are referred to by abbreviations L.1, L.2, and L.3 in figures of this section referring to layout 1, layout 2, and layout 3. Note that, the load points with dash lines in Fig. 6, are imaginary loads with a zero value.

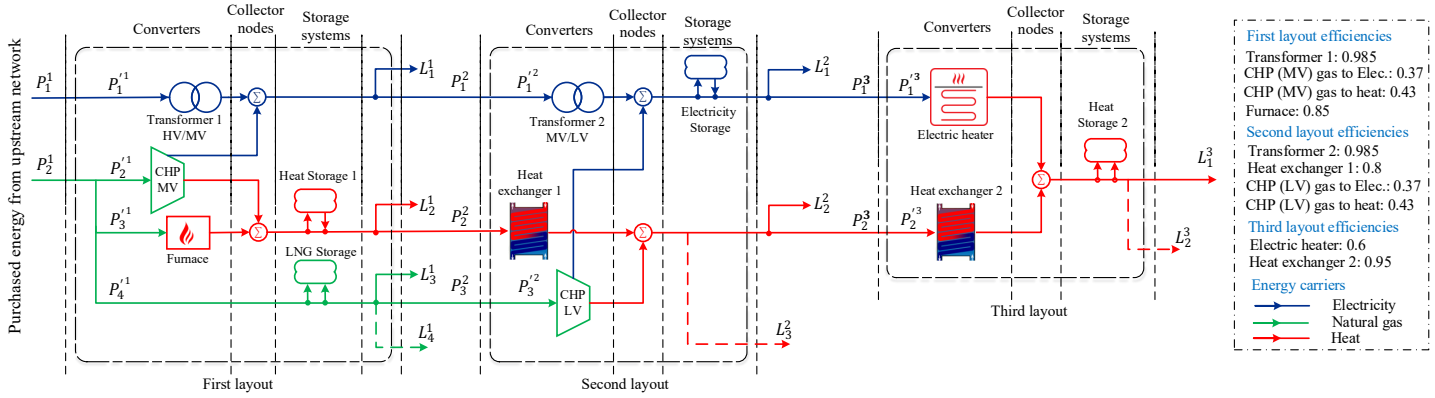

Fig. 6. Studied EHS and its characteristics.

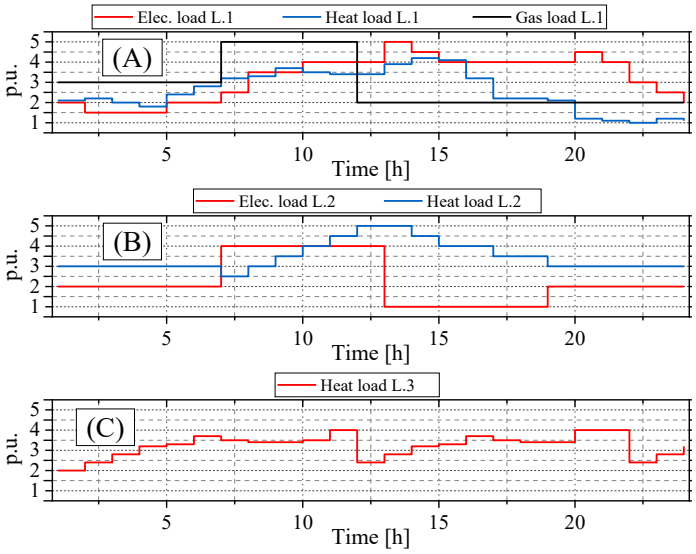

Fig. 7. Electricity, heat, and gas loads for each layout.

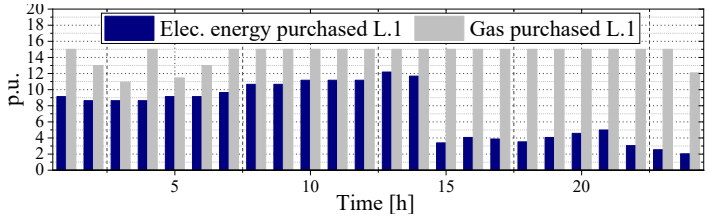

Fig. 8. Optimal input energy carriers to the first layout

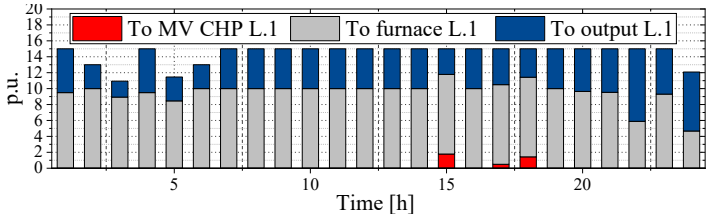

Fig. 9. Gas dispatch through the converters in the fist layout

The reason of adding these load points is to have a square matrix for $\boldsymbol{H^z}$ in the multi-layout EHS energy balance as $\boldsymbol{H^{z^{-1}}}$ is required. However, these load points do not affect the model as their values are set to zero. In the case study, there are six load points and two input energy prices which means there are eight uncertain parameters in each operating time slot (1 hour). Since the operation horizon is 24 hours, there are 192 ($24 \times 8 = 192$) uncertain parameters in the model. Simulations of this study have been conducted in GAMS software programing environment through BARON solver [32], on a computer with 8GB RAM and a Core-i7 CPU. The feasible region of the problem is convex.

B. *Robust Solutions*

Table I shows the total operation cost of the multi-layout EHS plant under uncertainty. These results are given for different values of uncertainty budget, i.e., $\Psi = 0 - 192$, and deviation range of uncertainties which is considered between 0% to 20% with 5% steps. Therefore, there are four cases for each deviation range including Case 1 with 5%, Case 2 with 10%, Case 3 with 15%, and Case 4 with 20% of deviation range. Based on Table I, it is observed that, $\Psi = 0$ stands as the deterministic representation of the proposed model, regardless of the deviation range of uncertain parameters. In fact, when $\Psi = 0$ no uncertain parameter can deviate from its estimate according to (5e). As the uncertainty budget Ψ increases, the value of objective function increases.

TABLE I

TOTAL OPERATION COST FOR EACH CASE WITH 24-STEP SIZE Ψ

Ψ	Total operation cost [$/day]			
	Case 1	Case 2	Case 3	Case 4
0	4163.565	4163.565	4163.565	4163.565
24	4298.780	4428.754	4558.804	4685.319
48	4396.473	4635.632	5445.665	6158.757
72	4481.046	5131.109	5851.964	6608.916
96	4553.941	5299.507	6147.385	7057.036
120	4603.074	5403.619	6329.170	7314.077
144	4640.044	5485.152	6606.242	7891.035
168	4665.404	5539.907	6726.981	8079.113
192	4681.307	5574.577	6781.069	8155.236

By increasing the deviation range in each case, the worst-case realization of uncertainties becomes worst and therefore the value of objective function increases again. The increase in the value of objective function is due to 1) increase of load resulting in more purchased energy at the first layout's input ports, 2) increase in the price of input energy carriers, and 3) unavoidable unsupplied load at each layout due to operating limitations.

Note that, the obtained solutions are also compared to the deterministic model in Table I where the deterministic model, i.e., with no uncertainty, has a value of objective function as 4163.565 $/day.

C. *ARMEO Operating Solutions for the First Layout (L.1)*

The operating solutions in this section are given based on, $\Psi = 120$ and 10% deviation range of uncertainties.

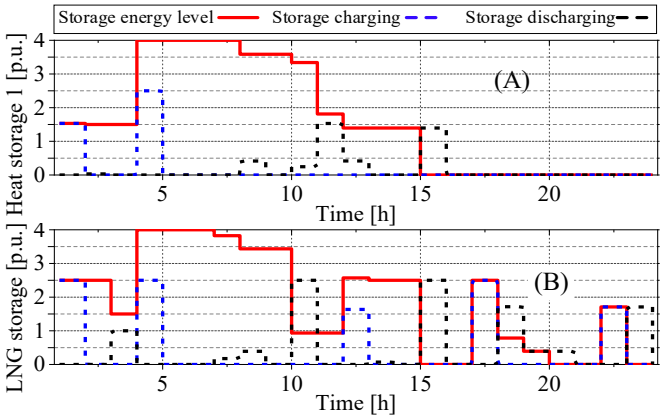

Fig. 10. Optimal storage operating solutions for the first layout

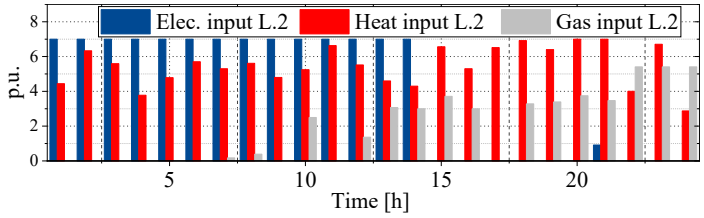

Fig. 11. Optimal input energy carriers to the second layout

The optimal purchased energy carriers from upstream network at the first layout's input ports is given by Fig. 8. As it is seen, the purchased electricity has considerably reduced between hours 15-20 which is due to the electricity peak price in these hours. In the opposite, the purchased gas has increased in electricity peak hours to compensate for the required electricity using CHP. The gas dispatch in the first layout supplies three two converters including the MV CHP, furnace as well as a straight path to the output loads. The gas dispatch between these paths is given by Fig. 9. As it is seen by Fig. 9, the majority of the input gas is used by furnace as it is responsible for meeting the heat load in both second and third layouts. The rest of the consumed input gas contributes to electricity and heat generation through MV CHP unit. The optimal operation of heat and LNG storage is also given by Fig. 10. These operating solutions are based on the optimal solutions obtained from solving the ARMEO problem.

D. ARMEO Operating Solutions for the Second Layout (L.2)

The second layout receives three input energy carriers from the first layout including electricity, heat, and gas to supply the second layout's loads on one hand, and deliver the required energy to the third layout, on the other hand. The optimal input energy carriers to the second layout (which form a part of the first layout's load) are given by Fig. 11. As it is seen, input electricity is approximately zero after hour 14 which is due to the dramatic reduction in electricity load in the second layout. The rest of the electric load after hour 14 is supplied by the LV CHP unit. For the same reason, the input gas has increased. The optimal operation of the electricity storage system is also given by Fig. 12. Accordingly, the storage system has contributed in optimal operation of the second layout by reasonable charging and discharging patterns which are inline by the load, and input energy of the second layout.

E. ARMEO Operating Solutions for the Third Layout (L.3)

The third layout includes two input energy carriers, i.e., electricity and heat, and one output heat load as well as a heat storage at the output port.

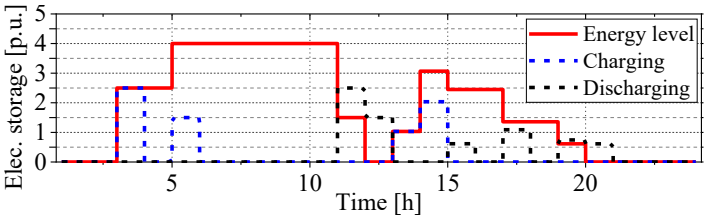

Fig. 12. Optimal storage operating solutions for the second layout

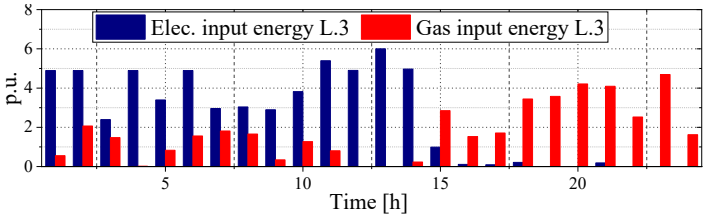

Fig. 13. Optimal input energy carriers to the third layout

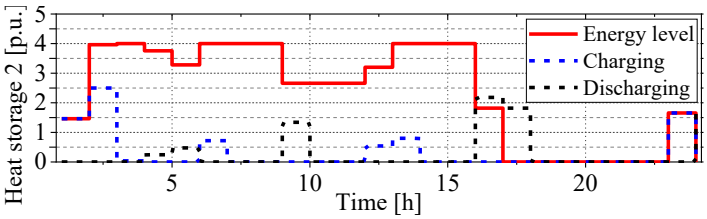

Fig. 14. Optimal storage operating solutions for the third layout

The electric heater and the heat exchanger are employed to supply the heat load. The input energy to the third layout (which forms a part of the second layout's load) is given by Fig. 13. The optimal operation of the heat storage 2 is also given by Fig. 14. Although the load level in the third layout does not have extreme changes, but the input energy patterns are subject to sudden changes, especially at hour 15. The reason is that the heat storage 2 reasonably discharges in hours 16 and 17 to supply the heat load and the rest of the load is met by the input heat from the previous layout.

F. Evaluating the Energy Balance throughout the Plant

The EHS in Fig. 6 includes three layouts. Each layout supplies its loads as well as the required energy by the next layout. The ARMEO model optimizes the operation of all layouts as a whole. Therefore, the interactions between layouts are considered to achieve a global optimal solution. This is because the energy balance of the multi-layout plant follows equation (4e) which provides the exact interactions between EHS layouts and their internal elements, i.e., converters and storages. The overall energy balance throughout the multi-layout EHS plant is given by Fig. 15. As it is seen, the input energy to each layout is based on both the load and the required energy at the next layout.

V. Conclusion

This paper presented a BCD robust model for managing multi-layout energy hub systems, as a new contribution to earlier studies, considering uncertainties of load and energy prices.

The concept of multi-layout energy hub was developed based on the conventional single-layout energy hub model. The proposed developed model was then solved through a new robust optimization model called BCD robust. A tri-level min-max-min robust optimization approach was developed to characterize uncertainties of load and energy prices in the proposed model. BCD method was employed to solve the inner max-min problem,

enabling the proposed model to characterize binary variables after uncertainty realizations, which was not applicable in previous RO applications.

Results showed that the model reasonably reduces the EHS input electricity in certain time periods and covered the required electricity with must-run processes by CHP unit, using natural gas. Moreover, it was evident that the operation of all layouts was based on a comprehensive optimization decision considering all layouts as a whole. This was reflected in Fig. 15 as well. In fact, it was shown that the optimality of operational decisions in each layout was dependent on the optimal decisions in another layout.

The proposed model can assist in the optimal operation of EHS facilities with different voltage levels and layouts. Our future work will focus on characterizing demand response schemes, such as emergency demand response in the proposed model.

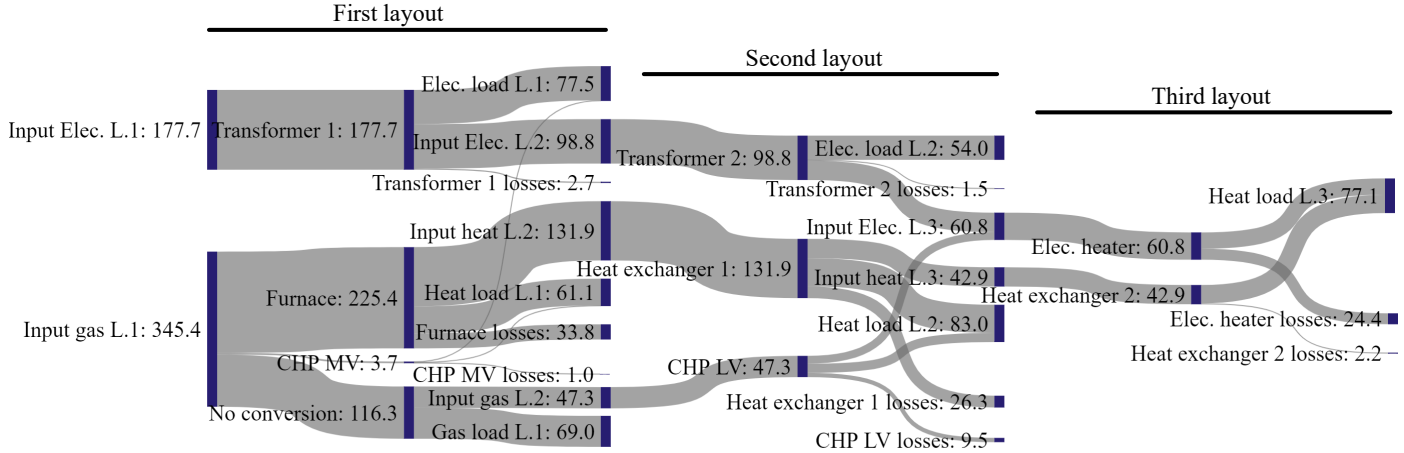

Fig. 15. Optimal energy balance throughout each layout and their associated elements

REFERENCES

[1] M. Geidl, G. Koeppel, P. Favre-Perrod, B. Klockl, G. Andersson and K. Frohlich, "Energy hubs for the future," in IEEE Power and Energy Magazine, vol. 5, no. 1, pp. 24-30, Jan.-Feb. 2007, doi: 10.1109/MPAE.2007.264850.

[2] M. Aghamohamadi, M. E. Hajiabadi, M. Samadi, "A novel approach to multi energy system operation in response to DR programs; an application to incentive-based and time-based schemes," Energy, Volume 156, 2018, Pages 534-547.

[3] M. Aghamohamadi, M. Samadi, I. Rahmati, "Energy generation cost in multi-energy systems; an application to a non-merchant energy hub in supplying price responsive loads," Energy, Volume 161, 2018, Pages 878-891.

[4] M. Geidl, and G. Anderson, "Optimal Power Flow of Multiple Energy Carriers," in IEEE Transactions on Power Systems, vol. 22, no. 1, pp. 145-155, Feb. 2007, doi: 10.1109/TPWRS.2006.888988.

[5] A. Heidari, R.C., "Bansal, Probabilistic correlation of renewable energies within energy hubs for cooperative games in integrated energy markets," Electric Power Systems Research, Volume 199, 2021.

[6] M. Aghamohamadi, M. Samadi, M. Pirnahad, "Modeling and Evaluating the Energy Hub Effects on a Price Responsive Load," IJEEE. 2019; 15 (1) :65-75

[7] S. Paudyal, C. A. Canizares, and K. Bhattacharya, "Optimal Operation of Industrial Energy Hubs in Smart Grids", in IEEE Transactions on Smart Grid, vol 6, no. 2, pp 684 – 694, Mar 2015, doi: 10.1109/TSG.2014.2373271.

[8] K. Kampouropoulos and F. Andrade, "Energy hub optimization applied on car manufacturing plants," 2016 IEEE ANDESCON, Arequipa, 2016, pp. 1-4, doi: 10.1109/ANDESCON.2016.7836236.

[9] Y. Zhang, X. Wang, J. He, Y. Xu, and W. Pei, "Optimization of Distributed Integrated Multi-Energy System Considering Industrial Process Based on Energy Hub," in Journal of Modern Power Systems and Clean Energy, vol. 8, no. 5, pp. 863-873, September 2020, doi: 10.35833/MPCE.2020.000260.

[10] Y. Huang, W. Zhang, K. Yang, W. Hou, and Y. Huang, "An Optimal Scheduling Method for Multi-Energy Hub Systems Using Game Theory," Energies, vol. 12, 2019, doi: https://doi.org/10.3390/en12122270

[11] R. Khezri, A. Mahmoudi and M. H. Haque, "A Demand Side Management Approach for Optimal Sizing of Standalone Renewable-Battery Systems," in IEEE Transactions on Sustainable Energy, doi: 10.1109/TSTE.2021.3084245.

[12] R. Khezri, A. Mahmoudi and M. H. Haque, "Optimal Capacity of Solar PV and Battery Storage for Australian Grid-Connected Households," in IEEE Transactions on Industry Applications, vol. 56, no. 5, pp. 5319-5329, Sept.-Oct. 2020, doi: 10.1109/TIA.2020.2998668.

[13] P. Emrani-Rahaghi, H. Hashemi-Dezaki,"Optimal Scenario-based Operation and Scheduling of Residential Energy Hubs Including Plug-in Hybrid Electric Vehicle and Heat Storage System Considering the Uncertainties of Electricity Price and Renewable Distributed Generations," Journal of Energy Storage, Volume 33, 2021, 102038.

[14] F. Niazvand, S. Kharrati, F. Khosravi, A. Rastgou, "Scenario-based assessment for optimal planning of multi-carrier hub-energy system under dual uncertainties and various scheduling by considering CCUS technology," Sustainable Energy Technologies and Assessments, Volume 46, 2021, 101300.

[15] M. H. Shams, M. Shahabi, M. Kia, A. Heidari, M. Lotfi, M. Shafie-khah, J. P.S. Catalão, "Optimal operation of electrical and thermal resources in microgrids with energy hubs considering uncertainties," Energy, Volume 187, 2019, 115949, ISSN 0360-5442.

[16] S. Hemmati, S.F. Ghaderi, M.S. Ghazizadeh, "Sustainable energy hub design under uncertainty using Benders decomposition method," Energy, Volume 143, 2018, Pages 1029-1047.

[17] A. J. Conejo, M. Carrión, and J. M. Morales, Decision Making Under Uncertainty in Electricity Markets. New York, NY, USA: Springer, 2010.

[18] S. A. Mansouri, A. Ahmarinejad, M. S. Javadi, J. P.S. Catalão, "Two-stage stochastic framework for energy hubs planning considering demand response programs," Energy, Volume 206, 2020, 118124, ISSN 0360-5442.

[19] J. Faraji, H. Hashemi-Dezaki, A. Ketabi, "Stochastic operation and scheduling of energy hub considering renewable energy sources' uncertainty and N-1 contingency," Sustainable Cities and Society, Volume 65, 2021, 102578, ISSN 2210-6707.

[20] P. Emrani-Rahaghi, H. Hashemi-Dezaki, A. Hasankhani, "Optimal stochastic operation of residential energy hubs based on plug-in hybrid electric vehicle uncertainties using two-point estimation method," Sustainable Cities and Society, Volume 72, 2021, 103059, ISSN 2210-6707.

[21] A. Dolatabadi, M. Jadidbonab and B. Mohammadi-ivatloo, "Short-Term Scheduling Strategy for Wind-Based Energy Hub: A Hybrid Stochastic/IGDT Approach," in IEEE Transactions on Sustainable Energy, vol. 10, no. 1, pp. 438-448, Jan. 2019, doi: 10.1109/TSTE.2017.2788086.

[22] T. Zhao, X. Pan, S. Yao, C. Ju and L. Li, "Strategic Bidding of Hybrid AC/DC Microgrid Embedded Energy Hubs: A Two-Stage Chance Constrained Stochastic Programming Approach," in IEEE Transactions on Sustainable Energy, vol. 11, no. 1, pp. 116-125, Jan. 2020, doi: 10.1109/TSTE.2018.2884997.

[23] G. Mohy-ud-din, D. H. Vu, K. M. Muttaqi, and D. Sutanto, "An integrated energy management approach for the economic operation of industrial microgrids under uncertainty of renewable energy," IEEE Trans. Ind. Appl., vol. 56, no. 2, pp. 1062–1073, Mar./Apr. 2020.

[24] P. Du, B. Li, Q. Zeng, D. Zhai, D. Zhou, and L. Ran, "Distributionally robust two-stage energy management for hybrid energy powered cellular networks," IEEE Trans. Veh. Technol., vol. 69, no. 10, pp. 12162–12174, Oct. 2020.

[25] A. Parisio, C. D. Vecchio, A. Vaccaro, "A robust optimization approach to energy hub management," International Journal of Electrical Power & Energy Systems, Volume 42, Issue 1, 2012, Pages 98-104.

[26] M. AkbaiZadeh, T. Niknam, A. Kavousi-Fard, "Adaptive robust optimization for the energy management of the grid-connected energy hubs based on hybrid meta-heuristic algorithm," Energy, Volume 235, 2021, 121171, ISSN 0360-5442.

[27] P. Zhao, C. Gu, D. Huo, Y. Shen and I. Hernando-Gil, "Two-Stage Distributionally Robust Optimization for Energy Hub Systems," in IEEE Transactions on Industrial Informatics, vol. 16, no. 5, pp. 3460-3469, May 2020, doi: 10.1109/TII.2019.2938444.

[28] R. Habibifar, M. Khoshjahan, V. S. Saravi and M. Kalantar, "Robust Energy Management of Residential Energy Hubs Integrated with Power-to-X Technology," 2021 IEEE Texas Power and Energy Conference (TPEC), 2021, pp. 1-6, doi: 10.1109/TPEC51183.2021.9384994.

[29] Z. Hashemi, A. Ramezani and M. P. Moghaddam, "Energy hub management by using decentralized robust model predictive control," 2016 4th International Conference on Control, Instrumentation, and Automation (ICCIA), 2016, pp. 105-110, doi: 10.1109/ICCIAutom.2016.7483144.

[30] B. Zeng and L. Zhao, “Solving two-stage robust optimization problems using a column-and-constraint generation method,” Operations Res. Lett., vol. 41, no. 5, pp. 457–461, 2013.

[31] M. Guzelsoy and T. K. Ralphs, “Duality for mixed-integer linear programs,” Int. J. Operations Res., vol. 4, no. 3, pp. 118–137, 2007.

[32] Kilinc, M. and N. V. Sahinidis, "Exploiting integrality in the global optimization of mixed-integer nonlinear programming problems in BARON," *Optimization Methods and Software*, 33, 540-562, 2018.